

Influence of fumed silica on the properties of cushion packaging materials based on bagasse pith and bisulfite spent liquor

Yanna Lv^{1,2*}, Beihai He^{1,3}, Yali Wu⁴

¹ State Key Laboratory of Pulping and Papermaking Engineering, South China University of Technology, 510640 Guangzhou, China

² Department of Media and Communication, Guangdong Industry Technical College, 510300 Guangzhou, China

³ National Engineering Research Center of Papermaking & Pollution Control, South China University of Technology, 510640 Guangzhou, China

⁴ Department of Food, Guangdong Industry Technical College, 510640 Guangzhou, China

Submitted May 1, 2014

In this work, biodegradable cushion packaging materials based on bagasse pith, magnesium bisulfite spent liquor and hydrophilic fumed silica were prepared via press-molding method and the effects of silica nanoparticles on the physical properties and biodegradation of the packaging materials were investigated. Results showed that the addition of silica nanoparticles increased the apparent density and the static compressive strength of bagasse pith cushion packaging materials. When the silica loading was within the critical value, the compressive strength was found to increase with the increase of specific surface areas of fumed silica due to a fine dispersion of nanofillers in the matrix. The morphology of fumed silica nanoparticles and the dispersion state of silica nanoparticles in the matrix were studied by transmission electron microscopy and scanning electron microscopy, respectively. The morphological analyses indicated that the reinforcement effect of fumed silica was the consequence of silica filler-matrix and silica filler-filler interactions. Biodegradation assays revealed that the presence of silica in the packaging materials reduced the biodegradation rate after 15 days of incubation in liquid nutrient medium.

Key words: Fumed silica, bagasse pith, cushion packaging material, biodegradation

INTRODUCTION

Cushion packaging materials protect fragile and delicate products against shock and vibration during shipping and handling. Generally, expanded polystyrene (EPS) and expanded polyethylene (EPE) are popular materials for this application due to their adequate mechanical strength and low cost. However, these foams are not biodegradable and recyclable, causing a serious white pollution. Therefore, manufacturers and consumers are looking for alternative materials that are eco-friendly and cheap, and possess good cushioning properties [1].

The biomass cushion packaging materials based on plant fiber have become a research hotspot all over the world due to their degradation and wide sources of raw materials. Many researchers have developed degradable cushion packaging materials with straw fibers (wheat straw fiber, rice straw fiber, bagasse fiber, rice husk fiber, etc.) [2-4]. Most of the research is still on laboratory level, and the

improvements in production technology and functional properties of materials will require further study.

Bagasse is a by-product of the sugarcane milling process and has adequate chemical and mechanical properties for paper making [5-7]. However, 30%–40% of the spongy structured bagasse pith in the sugarcane bagasse has adverse effect on the pulp quality; therefore, efficient removal of pith is a prerequisite in papermaking enterprise [8, 9]. In China, the annual output of sugar cane is 6 million tons, and the ratio of oven dry bagasse is about 13%, which means about 6.5 million tons [10]. The impressively abundant bagasse pith is mainly utilized as fuel for heating and power generation, but it can be used for more value-added products. Spongy bagasse pith has certain elasticity and resilience after being dried, thus, it can endow materials with good cushion performance without the need for foaming agents. The use of bagasse pith for producing biomass cushion packaging material is a way to enhance its added value.

Magnesium lignosulfonate, the major component of sulfite pulping waste liquor of sugarcane bagasse, is characterized by good

* To whom all correspondence should be sent:
E-mail: lvyanna2006@gmail.com

adhesion and degradability. The sugars and derivatives in the pulping waste liquor further enhance its adhesion ability via synergistic effect [11]. Therefore, acid sulfite pulping waste liquor can be used as an adhesive mixed with bagasse pith to produce degradable cushion packaging materials.

Some researchers compounded plant fibers with biodegradable adhesives to produce biodegradable packaging materials. Studies showed that high plant fiber fractions can help reduce the cost per unit volume of packaging materials. However, the strength of the materials consequently decreases [12, 13]. Therefore, fumed silica is selected as the reinforcing filler of the bagasse pith cushion packaging materials in this experiment. Fumed silica (SiO_2) is usually employed as an enhancing agent in thermoplastic polymers and rubber to increase their mechanical properties, such as toughness and tensile strength. Bouaziz et al. [14] reported the reinforcement mechanism of SiO_2 in polypropylene composites. Zhang and coworkers [15] studied the impact of silica content on tensile modulus and impact strength of high-density polyethylene. Prasertsri and Rattanasom [16] investigated the effects of loading and surface area of fumed silica on stiffness and tear strength. As far as we are aware, however, no work has been done on the reinforcement by fumed silica of plant fiber-based materials.

Therefore, this study aims to prepare cushion packaging materials based on bagasse pith, magnesium bisulfite spent liquor, and fumed silica via press-molding process and to investigate the effects of fumed silica on the physical and mechanical properties of the cushion packaging materials. The biodegradation of the specimen is also reported in this paper. Interfacial studies were made with scanning electron microscopy (SEM) to illustrate the silica reinforcement mechanism.

MATERIALS AND METHODS

Experimental equipment design

The experimental equipment for preparing the biodegradable cushion packaging materials (BCPMs) used in this study was designed by Tianjin Sichuang Jingshi Technology Co. Ltd. (Tianjin, China). The equipment consists of top pressure plate, lower pressure plate, inner mold, and outer mold. During drying, water in packaging materials evaporated from the small holes in the copper mesh. The outer mold is made of 3 mm-thick stainless steel plates to ensure the shape of the inner mold.

Materials and chemicals

The bagasse pith with 13.36% moisture content and the spent liquor with 52% solid content were supplied by Jiangmen Sugarcane Chemical Factory (Group) Co. Ltd. (Guangdong, China). The fraction of bagasse pith passing a 10-mesh sieve was used in all experiments. The spent liquor from the magnesium bisulfite pulping process of bagasse was used as the adhesive.

Analytical-grade sodium hydroxide was purchased from Guangzhou Chemical Reagent (Guangdong, China) and was used for pH adjustment. Three types of hydrophilic fumed silica nanoparticles from Guangzhou GBS High-Tech & Industry Co. Ltd. (Guangdong, China), were used as reinforcing filler. These three types were HL150, HL200 and HL380 with nominal SSAs of 150, 200 and 380 $\text{m}^2 \text{g}^{-1}$, respectively. The physical and chemical properties of silica are shown in Table 1. The surface area and porosity measurements were performed using an ASAP 2020 (Accelerated Surface Area and Porosimetry) machine. Surface properties were evaluated through nitrogen gas physisorption process. The SSA of the fumed silica was calculated according to the Brunauer-Emmett-Teller (BET) procedure [17]. The surface area contribution according to pore dimensions was also determined according to the Barrett-Joiner-Holenda (BJH) method [18].

In the following discussion, the cushion packaging materials are labeled referring to the name of silica nanoparticle and its weight content. For example, pith-HL200-1 indicates that pith and 1 wt% HL200 were used as matrix and filler, respectively.

Preparation of the BCPMs

The BCPMs were manufactured on the basis of previous results [19]. The solid content of the spent liquor was 52%, and the mass ratio of bagasse pith to bisulfite spent liquor (on solid content basis) was 2:1. The amount of lignin sulfonate in the adhesive was determined by its solid content. Under certain experimental conditions, BCPMs had a low apparent density, the lowest water absorption capacity and good mechanical properties.

The magnesium bisulfite spent liquor (pH 4.5) was placed in a plastic beaker. Then, sodium hydroxide was added until the spent liquor became neutral which ensured that the cushion packaging materials could be directly contacted with the packaged articles. Finally, silica (1%-15% relative to oven dry bagasse pith) was charged to the neutralized spent liquor for filler dispersion. The mixed solution and the bagasse pith were stirred

together for 2 min in the SHR-10A high-speed mixer (Zhangjiagang Gelan Machinery Co., Ltd., China). The homogeneously blended ingredients were discharged to the molds and compressed by a Micro press machine. The materials were processed at a set pressure of 52KPa and time of 30 s. After the molding process, the materials in the inner molds were dried at $155 \pm 2^\circ\text{C}$ for 45 min in an air oven. Eventually, the BCPMs were obtained after demolding.

Table 1. Physical and chemical properties of fumed silicas.

Sample	BET surface area (m^2g^{-1})	BJH adsorption cumulative surface area of pores (1.7-300nm)(m^2g^{-1})	pH value
HL150	138.6± 1.1	106.8	4.33
HL200	154.4± 1.1	119.9	4.83
HL380	325.5± 2.6	246.3	4.17
HL150	138.6± 1.1	106.8	4.33

BCPMs biodegradability

Biodegradability of BCPMs was characterized by the weight-loss method [20]. Table 2 shows the reagents and dosages to confect the mineral salt medium (MSM).

The ingredients of a medium developed for screening of BCPMs strain were bagasse pith and MSM. Solid media were prepared by the addition of 1.5% agar to the above mentioned medium. Soils from Jiangmen Sugarcane Chemical Factory (Group) Co. Ltd, the lotus pond of the campus as well as the surrounding area of the waste plants were taken as samples, which were transferred into a shake flask containing MSM medium. The fungal strains were domesticated at 30°C and 150 rpm for 5 days in MSM medium with bagasse pith as the sole carbon source. After that, the MSM plate was coated by the dilution coating method using bagasse pith as the sole carbon source. Five strains were selected from colonies growing faster and in good condition, and then were streaked onto the MSM plate. Finally single colonies were inoculated on the slant and prepared for the determination of degradation rate.

Table 2. Reagents and dosages to confect the MSM.

Reagent	Dosage (g)	Reagent	Dosage (g)
NaCl	1.0	$(\text{NH}_4)_2\text{SO}_4$	2.0
K_2HPO_4	1.0	$\text{MnCl}_2 \cdot 7\text{H}_2\text{O}$	0.001
MgSO_4	1.0	$\text{ZnSO}_4 \cdot 7\text{H}_2\text{O}$	0.001
CaCO_3	2.0	$\text{FeSO}_4 \cdot 7\text{H}_2\text{O}$	0.001

Weight-loss method was applied to determine BCPMs degradation rate. First, BCPMs liquid medium was prepared and discharged into three

250 mL Erlenmeyer flasks, respectively. The liquid was sterilized under 0.105 MPa for 30 min. Under aseptic operational conditions, the strains were selected from the slant mentioned above, then inoculated into the prepared medium and incubated for 15 days at 30°C and 150 rpm. The BCPMs which were not degraded were separated from the Erlenmeyer flask by filtering. The samples were purified with distilled water and then dried to constant weight at 60°C in an air oven. Afterwards, the mass of the samples after degradation was weighed, and the weight loss of BCPMs before and after degradation was calculated. The degradation rate of BCPMs can be converted to the weight-loss rate [21]. The weight loss rate is described by Eq. (1).

$$W = \frac{m_1 - m_2}{m_1} \times 100\% \quad (1)$$

where W is the degradation rate, m_1 is the mass of the samples before degradation, m_2 is the mass of the samples after degradation.

BCPMs characterization

Apparent density. The length, width and thickness of the samples were measured with a manual vernier caliper (Guanglu, China). The apparent density was calculated as the relationship between weight and volume according to the GB8168-2008 Testing Method of Static Compression for Packaging Cushioning Materials. The reported values are the averages of six determinations for each formulation.

Mechanical properties. The mechanical properties of the samples were investigated through static compression tests. The tests included compressive stress-strain (σ - ϵ) and static cushion factor-strain evaluations. Static compression tests were performed according to GB8168-2008 on five specimens that were stored for 24 h at $23 \pm 2^\circ\text{C}$ and $50 \pm 2\%$ relative humidity using a CMT4204 universal testing machine (MTS China Co. Ltd.) operated at a speed of 12 ± 2 mm/min.

TEM analysis

The particle sizes and morphologies of silica were examined by transmission electron microscopy (TEM, JEOL JEM-2010HR). Samples were prepared by placing droplets of a suspension of silica powders in anhydrous alcohol on copper grids.

SEM analysis

The morphologies of BCPMs before and after degradation were characterized by field emission scanning electron microscopy (SEM, FEI Quanta

400F). The fracture surfaces of samples were coated with gold using a vacuum sputter-coater before observation.

RESULTS AND DISCUSSION

TEM analysis of fumed silica

Fig. 1 presents TEM micrographs of three kinds of fumed silica used in this study. It was found that fumed silica nanoparticles were sphere shaped and connected as grape bunches. Nanoparticles were prone to agglomerate due to hydrogen bonds between the surface hydroxyl groups of silica. The forces between the agglomerates were easily destroyed using mechanical agitation and the aggregation process was reversible [22].

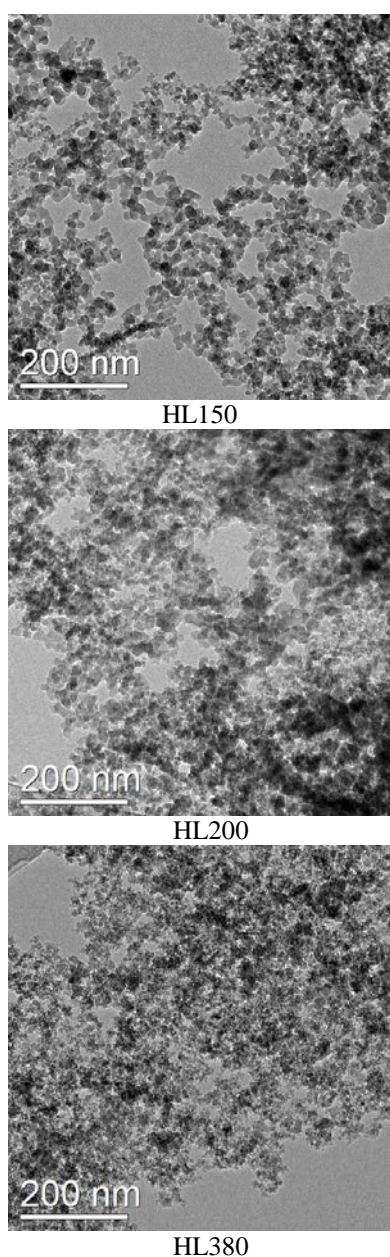


Fig. 1. TEM micrographs of fumed silica nanoparticles.

The dispersion of fumed silica in the polymer matrix affected the mechanical behavior of the resulting composites.

The particle size of silica could be indirectly reflected from the specific surface area (S_{BET}). Small diameter particles had high specific surface area. TEM analysis showed that the mean diameter of HL150, HL200 and HL380 ranged from 10 to 18 nm, 8 to 14 nm and 4 to 10 nm, respectively, consistent with S_{BET} test results.

Apparent densities of BCPMs

The apparent densities of BCPMs with different silica loadings are shown in Fig. 2. It is seen that cushion packaging materials with silica have higher apparent densities compared with materials without silica, which was 0.204 g/cm^3 [19]. The apparent densities of BCPMs increased with the increasing silica loading.

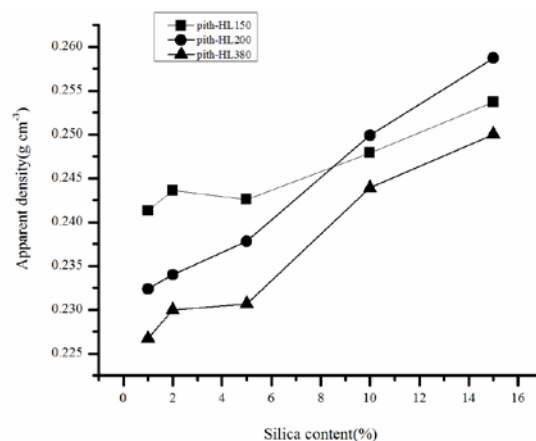


Fig. 2. Effects of silica loadings on BCPMs apparent densities.

Given the same silica loading, BCPMs with HL380 reinforcement has the minimum apparent density. Compared with HL150 and HL200, HL380 has the largest specific surface area, more silanol groups (Si-OH) on the surface, more additional cross-linking reactions produced from the chemical reaction with phenolic hydroxyl groups (Ph-OH) and sulfonic groups in the molecular chains of magnesium lignosulfonate, and higher network strength of the reinforcement system. Therefore, HL380 underwent the minimum volume deformation under same molding pressure of 52 KPa. When silica loading exceeded 10 wt%, BCPMs with HL200 reinforcement achieved higher apparent density than BCPMs with HL150 reinforcement. This finding may be ascribed to maximum volume deformation of BCPMs with HL200 reinforcement under external forces.

The number of silanol groups in HL200 was greater than in HL150. In addition, the interparticle interaction of HL200 was stronger than that of

HL150. Therefore, HL200 particles were prone to agglomerate as the amount of the particles increased [23]. The HL200 aggregates yielded a poor dispersion within the bagasse pith/ bisulfite spent liquor matrix and led to more matrix defects. Poor dispersion and matrix defects could lower the effective stress transfer at the interface and cause large volume deformation of BCPMs. In the experiment, the loadings of fumed silica increased from 1 wt% to 15 wt%, whereas the apparent density of BCPMs varied from 0.22 g/cm³ to 0.26 g/cm³. The addition of lightweight amorphous silica powder had little effect on the apparent density of BCPMs. Fumed silica is beneficial for maintaining the low apparent density of cushion packaging material.

Mechanical properties of BCPMs

Effect of silica loading. To analyze the effect of silica loading on the cushion performance of BCPMs, 1 wt% HL150, HL200 and HL380 silica were added to the samples. The corresponding static compressive stress-strain curves are shown in Fig. 3.

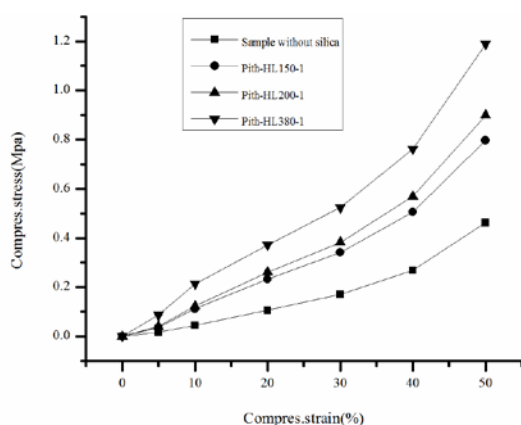


Fig. 3. Static compression properties of BCPMs with and without silica.

BCPMs without silica can withstand stress of 0.17 MPa, whereas BCPMs with HL150, HL200 and HL380 can withstand stress of 0.31MPa, 0.36MPa and 0.48 MPa, respectively, under the same strain of 30%. This finding indicates the significant effect of silica loading in improving the compression strength of BCPMs. The stress-strain diagram shows that under the same strain conditions, stress increased at first and then decreased with the increase in silica loadings. Such variation in trend can be analyzed qualitatively based on the microstructure of the interface between silica and adhesive. Magnesium lignosulfonate is the major component of bisulfate spent liquor serving as the adhesive in this experiment. The molecules of lignosulfonate

contain various active functional groups such as hydroxyl groups (including alcoholic hydroxyl groups and phenolic hydroxyl groups), sulfonic groups, and carboxy groups [24] that can combine with silanol groups on the silica surface to develop chemical bonds, and enhance the binding between nanoparticles and adhesive. The increase of silica loading may contribute more silanol groups to the system and expand the contact area with pulping spent liquor, developing more cross-linking joints, which is good for stress transfer. Thus, the load capacity of the adhesive membrane formed on the surface of the material finally increased. The effects of silica loading on the static compressive stress-strain curve of BCPMs were studied under the same specific surface area (S_{BET}) of fumed silica. The results are shown in Fig. 4.

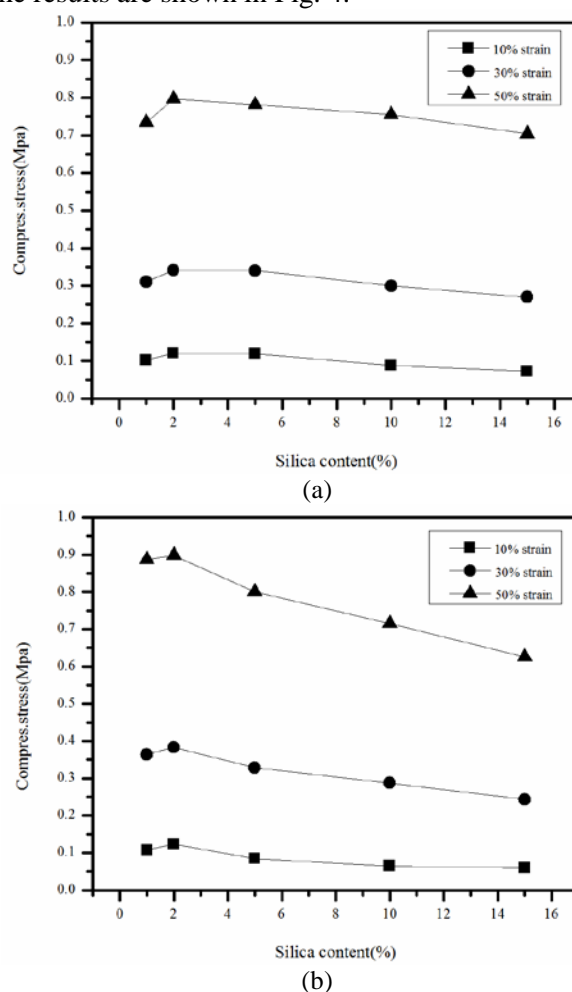


Fig. 4. Static compression properties of BCPMs filled with different silica loadings: (a) HL150; (b)HL200.

By contrast, less than 5 wt% HL150 and less than 2 wt% HL200 served as inorganic rigid fillers scattered evenly in the bagasse pith and spent liquor compound, which can expand the region of stress concentration and absorb certain deformation, thus increasing the compressive stress. Given that silica

was dispersed in the pulping spent liquor first in this experiment, the silica-adhesive interfacial adhesion was improved with the increase in silica loading. However, excessive silica loading may lead to bigger sizes of the agglomerates in the adhesive, which increases the defects of BCPMs, thus decreasing compressive stress accordingly.

The comparison of drop points in Figs. 4(a) and 4(b) showed that BCPMs with higher than 2 wt% HL200 silica as reinforcing filler have poor mechanical properties, which are caused by the agglomeration of HL200 with high surface energy. The result is similar to the observations reported by Kantala et al. [22].

Effect of silica specific surface area.

Specific surface area is one of the most important morphological parameters of fumed silica without surface modification [23]. The effects of S_{BET} on the cushioning property of BCPMs were studied under the same silica loading conditions. The results are displayed in Fig.5.

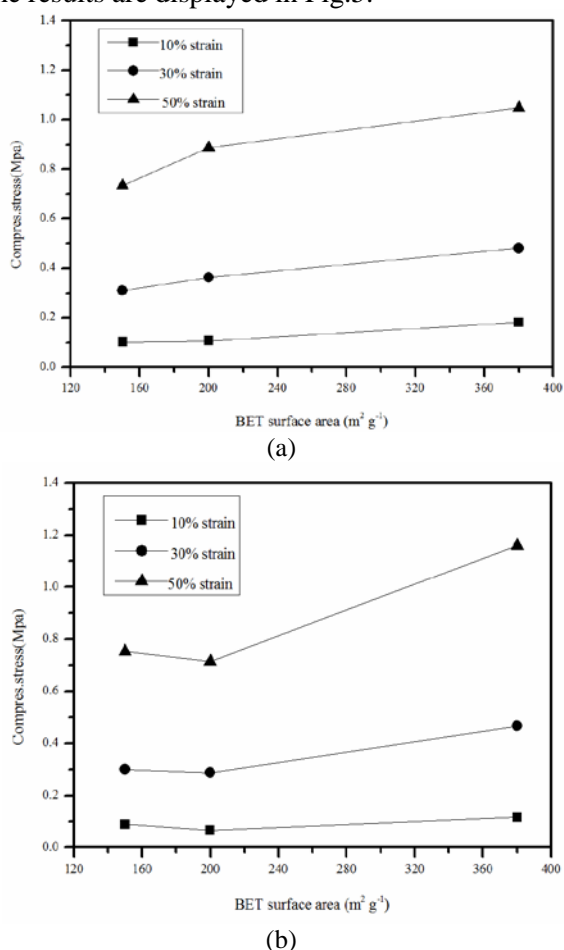


Fig. 5. Static compression properties of 1 wt% (a) and 10 wt% (b) filled BCPMs with various silica S_{BET} .

As shown in Fig. 5, stress of BCPMs containing 1 wt% silica increased with the increase of silica contents. A further increase in compression strength

was observed under high compressive strain condition. When S_{BET} of silica increased from 200 to 380 m² g⁻¹, the compressive stress increased by 0.08MPa with the strain of 10%, 0.12MPa with the strain of 30% and 0.16MPa with the strain of 50%. This is probably due to the increased interfacial area between adhesive and silica nanoparticles with high S_{BET} value. Nevertheless, when the silica loading was up to 10 wt%, BCPMs with HL200 reinforcement can withstand less stress than HL150. The results showed that once silica loading exceeded the critical value, the filler-filler interaction was dominant, which resulted in weak interactions between silica particles and matrix. The compression strength of BCPM decreased in its macro performance.

The cushion factor-maximum static stress curves of BCPMs with three kinds of silicas are presented in Fig.6. The specific surface area of silica had a significant effect on the cushioning properties of BCPMs. Higher S_{BET} values resulted in a higher cushion factor, revealing that the BCPMs became stiffer.

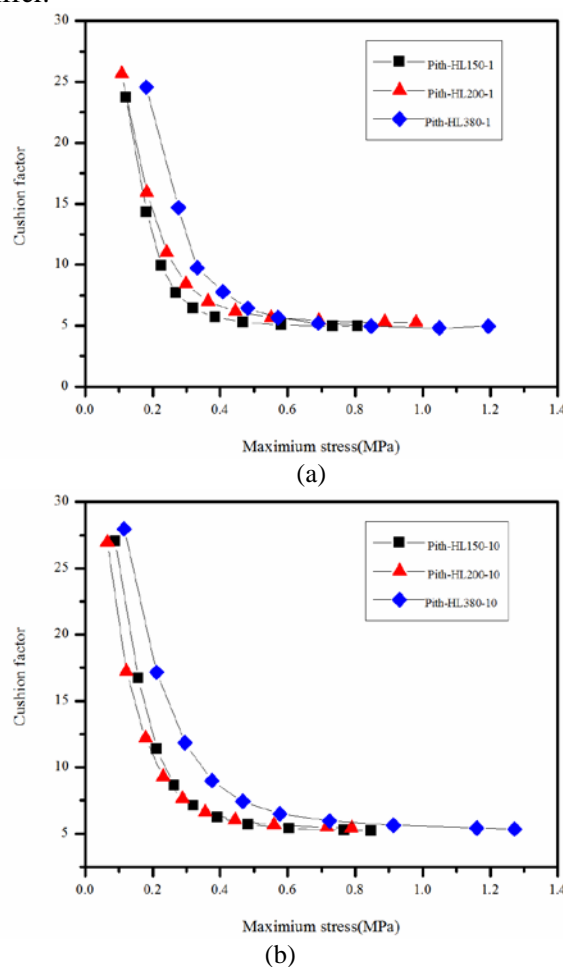


Fig. 6. Static cushion factors of 1 wt% (a) and 10 wt% (b) filled BCPMs with various silica S_{BET} .

Compared with high-density EPS with apparent density of 0.0226 g/cm^3 , BCPMs display a lower cushion factor under high compressive stress ($>0.4 \text{ MPa}$), and perform well in a more extensive stress range [25]. These data indicate that better protection and lower BCPMs consumption could be achieved in packing heavy fragile articles. In addition, BCPMs is superior to nondegradable EPS with respect to mechanical and electronic products as well as large household appliances.

SEM Analysis

The morphology of BCPMs was studied by SEM in order to evaluate the dispersion state of silica particles in the bagasse pith/ bisulfite spent liquor matrix. The particles observed in Fig.8 and Fig.9 are fumed silica.

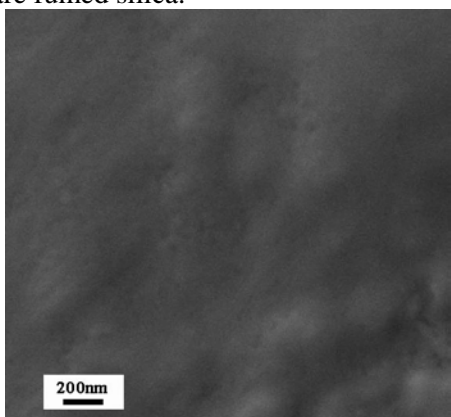


Fig. 7. SEM micrographs of BCPMs without silica.

It can be seen from Fig. 7 that the surfaces of BCPMs are covered by a layer of dense membrane from magnesium bisulfate spent liquor. The fumed silica particles are dispersed into the adhesive membrane. Therefore, the compressive stress was transferred from the membrane onto the rigid phase [14], and fumed silica particles reinforced the BCPMs. The increase of S_{BET} led to bigger sizes of the agglomerates. By comparing the images in Figs. 8 and 9, it can be seen that the size of HL200 agglomerates is larger than that of HL150.

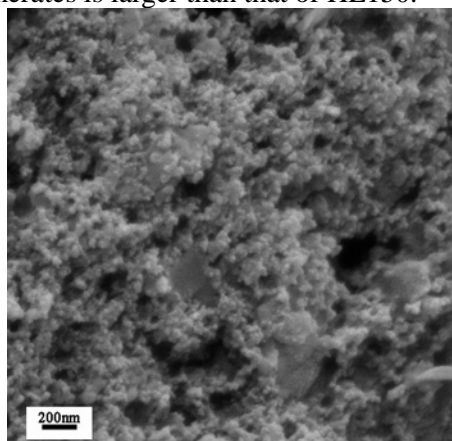


Fig. 8 SEM micrographs of BCPMs with 10 wt% HL150.

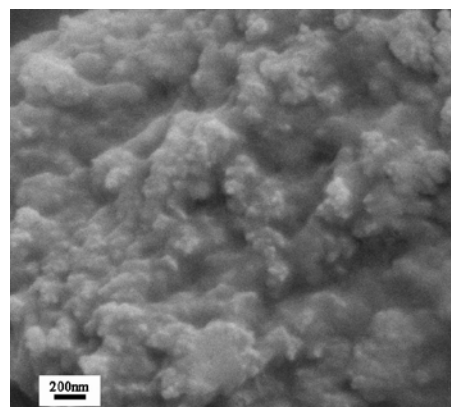


Fig. 9. SEM micrographs of BCPMs with 10 wt% HL200.

These silica agglomerates became the stress concentration points as the BCPMs were compressed, making the BCPMs more prone to damage. This finding is in accordance with the change trend of the mechanical properties of BCPMs.

Biodegradation

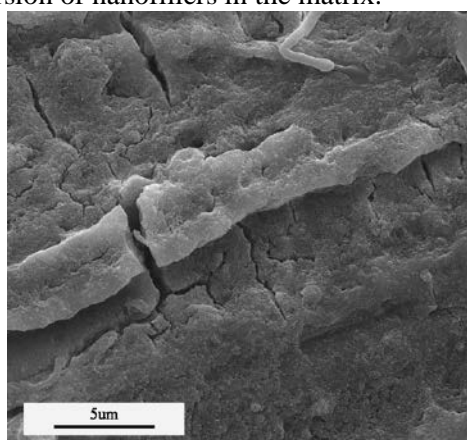
Previous studies have proved that there were large amounts of hemicellulose in bagasse pith and the degradation of hemicellulose mainly makes use of molds [26]. In the experiment, the samples were cultured with molds for 15 days in submerged culture with shake flask, and then the biodegradation rate of BCPMs was measured by the weight-loss method. The weight loss was observed for the BCPMs without silica and with 10 wt% HL200 (52.5% and 45.7%, respectively) after 15 days. The presence of silica particles in the BCPMs reduced the biodegradation rate. The BCPMs with 10 wt% HL200 were left to dry in an air oven at $60 \text{ }^\circ\text{C}$ after degradation, and then the degradation state was observed by SEM.

The SEM micrographs of the BCPMs surfaces before and after degradation treatment are shown in Fig. 10. The micrographs clearly show that the surfaces of the BCPMs are covered by a film formed by the adhesive before degradation treatment. The film was dense and thick. After degradation treatment, the BCPMs became thinner, and the surface was dotted by different-sized holes because of erosion.

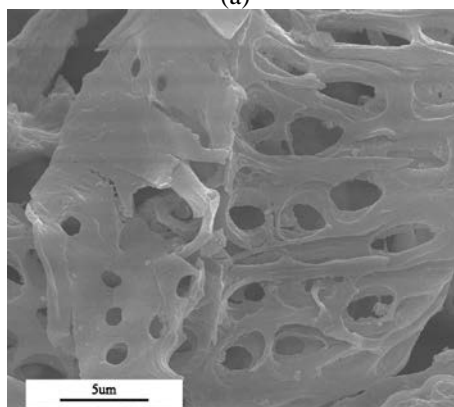
CONCLUSIONS

Biodegradable cushion packaging materials based on bagasse pith, magnesium bisulfite spent liquor and hydrophilic fumed silica were prepared via press-molding method. The experimental results revealed that the dispersion of fumed silica within the matrix and the size distribution of silica nanofiller aggregates had a significant effect on the

properties of BCPMs. The apparent densities of BCPMs increased with the increase of silica loading. Given the same silica loading, BCPMs reinforced by the silica with largest specific surface area has minimum apparent density. From the study of the cushioning properties, it was found that the addition of fumed silica improved the compression strength of BCPMs. However, excessive silica loading may lead to bigger sizes of the agglomerates in the adhesive, which increases the defects of BCPMs, thus decreasing compressive stress accordingly. When the silica loading was within the critical value, the compressive strength was found to increase with the increase of specific surface areas of fumed silica due to a fine dispersion of nanofillers in the matrix.



(a)



(b)

Fig. 10. SEM micrographs of BCPMs surface: (a) before degradation treatment (b) after degradation treatment.

The morphological analyses indicated that the reinforcement effect of fumed silica was the consequence of silica filler-matrix and silica filler-filler interactions.

BCPMs had good cushioning properties within a large stress range, and good degrading performance in mold conditions. Compared with high-density EPS, BCPMs can be used for packing heavy delicate articles.

Acknowledgements: The authors wish to thank the Guangzhou GBS High-Tech & Industry Co., Ltd. for offering hydrophilic fumed silica nanoparticles.

REFERENCES

1. Y. Chen, Z.Y. Zhang, Y. Ishikawa, T. Maekawa, *Trans. ASAE*, **45**, 1051 (2006).
2. S. Shibata, Y. Cao, I. Fukumoto, *Polym. Compos.*, **26**, 689 (2005).
3. L. K. Chen, Q. F. Zhang, Z. F. Lei, Y. H. Wang, X. L. Dong, *Packaging Engineering*, **32**, 11 (2011). (in Chinese)
4. F. Y. Li, K. K. Guan, P. Liu, G. Li, J. F. Li, *Int. J. Polymer Sci.*, **70**, 1 (2014).
5. R.K. Sharma, K.R. Yadav, V.L. Maheshwari, R.M. Kothari, *Crit. Rev. Biotechnol.*, **20**, 237 (2000).
6. S. Hedjazi, O. Kordsachia, R. Patt, A. Latibari, U. Tschirner, *Holzforchung*, **62**, 142 (2008).
7. A. Khakifirooz, F. Ravanbakhsh, A. Samariha, M. Kiaei, *BioResources*, **8**, 21 (2013).
8. J. A. Lois-Correa, *Ingeniería Investigación y Tecnología*, **13**, 417 (2012).
9. S.K. Paul, K.S. Kasiviswanathan, *Ippta*, **10**, 1 (1998).
10. H. Y. Zhan, *China Pulp and Paper*, **29**, 56 (2010). (in Chinese)
11. H.H. Nimz, *Wood Adhesives Chemistry and Technology*, A. Pizzi, (ed.), Marcel Dekker, New York. (1983).
12. J.E. Van Dam, M.J. van den Oever, E.R. Keijsers, J.C. van der Putten, C. Anayron, F. Josol, A. Peralta, *Ind. Crop. Prod.*, **24**, 96 (2006).
13. S. Shibata, *BioResources*, **7**, 5381 (2012).
14. A. Bouaziz, M. Jaziri, F. Dalmas, V. Massardier, *Polym. Eng. Sci.*, **54**, 2187 (2014).
15. M. Q. Zhang, M. Z. Rong, H. B. Zhang, K. Friedrich, *Polym. Eng. Sci.*, **43**, 490 (2003).
16. S. Prasertsri, N. Rattanasom, *Polym. Test.*, **31**, 593 (2012).
17. S. Brunauer, P.H. Emmett, E. Teller, *J. Am. Chem. Soc.*, **60**, 309 (1938).
18. E. Barret, L. Joyner, P. Holenda, *J. Am. Chem. Soc.*, **73**, 373 (1951).
19. Y.N. Lv, J. Z. Ou, K. J. Chen, The Second International Papermaking and Environment Conference, W, L.J., Ni, Y.H., Hou, Q.X., and Liu, Z. (eds.), China Light Industry Press, Bei Jing. (2009).
20. F. Li, H. Yang, Z.Q. Guo, Z.Y. Wang, Y. Wang, D.B. Liu, H.M, Xia, S. Chen, *Journal of Northeastern University*, **43**, 127 (2011).
21. H.J. Hou, F.S. Chen, X.L. Cheng, B.W. Gong, *Plastics Science and Technology*, **37**, 40 (2009).

- 22.C. Kantala, E. Wimolmala, C. Sirisinha, N. Sombatsompop, *Polym. Adv. Technol.*, **20**, 448 (2009).
- 23.M. J. Wang, M.D. Morris, Y. Kutsovsky, *Kautschuk, Gummi & Kunststoffe*, **61**, 107 (2008).
- 24.D. J. Yang, Y. G. Du, J.G. Fu, X. Q. Qiu, *CIESC J.*, **61**, 1859 (2010).
- 25.C. Liu, Y. D. Ren, *Packaging Engineering*, **31**, 117 (2010).
- 26.R.Sanzjuan, J.Anzaldo, J.Vargas, J.Turrado, R.Patt, *Eur. J. Wood & Wood Prod.*, **59**, 447 (2001).

ВЛИЯНИЕ НА ОПУШЕН СИЛИЦИЕВ ДИОКСИД ВЪРХУ СВОЙСТВАТА НА МЕКИ ОПАКОВЪЧНИ МАТЕРИАЛИ НА ОСНОВАТА НА СЪРЦЕВИНА ОТ БАГАСА И БИСУЛФИТНА ОТПАДЪЧНА ЛУГА

Янна Лв^{1,2*}, Бейхай Хе^{1,3}, Яли У⁴

¹ Държавна лаборатория по инженерство на целулозата и хартията, Южен китайски технологичен университет, Гуанчжу, Китай

² Департамент по медии и съобщения, Технически колежпромишлено-технически колеж Гуандонг, Гуанчжу, Китай

³ Национален инженерно-изследователски център по хартия и контрол на замърсяванията, Южен китайски технологичен университет, Гуанчжу, Китай

⁴ Департамент по храните, Технически колежпромишлено-технически колеж Гуандонг, Гуанчжу, Китай

Постъпила на 1 май, 2014 г.

(Резюме)

В настоящата работа се съобщава за биоразградими опаковъчни материали, основани на сърцевината от багаса, отпадъчна бисулфитна луга, съдържаща магнезий и хидрофобен опушен силициев диоксид. Материалите са приготвени чрез леене под налягане. Изследван е ефектът на добавените наночастици от силициев диоксид върху физичните свойства и биодеградационните отнасяния. Резултатите показват, че добавянето на наночастици от силициев диоксид повишава привидната плътност и здравината към статично свиване на меки опаковъчни материали от сърцевина на багаса. Когато натоварването със силициев диоксид е в границите на критичните стойности, здравината на свиване расте с нарастването на специфичната повърхностна площ на опушения силициев диоксид поради фината дисперсия от наночастици в матрицата. Морфологията на наночастиците от опушения силициев диоксид и на дисперсионното им състояние са изучени с трансмисионна и сканираща електронна микроскопия. Морфологичните анализи показват, че ефектът на усилване от опушения силициев диоксид е в следствие на взаимодействия пълнеж-матрица и пълнеж-пълнеж. Пробите показват, че в присъствие на силициев диоксид в опаковъчните материали, тяхната биоразградимост намалява след престой от 15 дни в течна хранителна среда.